2011 IEEE/RSJ International Conference on
Intelligent Robots and Systems
September 25-30, 2011. San Francisco, CA, USA

On On-Orbit Passive Object Handling by Cooperating Space Robotic Servicers

Georgios Rekleitis and Evangelos Papadopoulos, *Senior Member, IEEE*

Abstract—**Space exploitation will require efficient techniques for manipulating passive objects on-orbit. This work presents a manipulation technique that utilizes both on-off thrusters and manipulator proportional forces to handle passive objects on orbit, canceling the effect of limit cycles on the objects. The system dynamics including the unilateral constraints and the on-off thrusting are discussed. Using a two-layer optimization process, a planning strategy for the trajectory tracking motion of a passive object including optimal end-effector contact point selection, is developed. The manipulation strategy is illustrated using a 3D scenario. A model-based controller adapted to the special characteristics of the system is presented and its response is discussed. The performance of the proposed manipulation system is shown to be promising, while it reduces excessive thruster fuel consumption.**

I. INTRODUCTION

On-Orbit Servicing (OOS) is a relatively new but growing area of space activities, requiring systems capable of fulfilling tasks such as construction, maintenance, astronaut assistance, docking and inspection, or even orbital debris handling and disposal. Some of these tasks can be performed by astronauts in Extra Vehicular Activities (EVA); however, in general these are dangerous tasks and subject to limitations such as the magnitude of a force/ torque an astronaut can apply, motions that can be performed, or even EVA time limitations. To relieve astronauts from EVA, enhance EVA performance and expand the EVA with tasks that astronauts cannot perform, robotic systems acting as orbital servicers will be required.

During the last two decades, robotic OOS has been discussed and a number of architectures have been proposed [1]. Important robotic tasks, such as orbital assembly, debris handling etc., require passive object handling capabilities. To handle a passive object, a secure and firm grasp is needed. Several approaches have been proposed [2, 3], some of which have been tested experimentally, [4, 5]. However, issues such as the handling of large objects, remain open. On-orbit object handling has similarities to cooperative manipulation of passive objects on earth [6], with the additional complexities that in space no fixed ground to support the manipulators exists and that the development of propulsion forces depends on on-off thrusters.

Although several prototype robotic servicers have been proposed and studied since the 1990's [4, 5, 7, 8], there are only a few studies concerning the dynamics and control of the motion of an already grasped body. Dubowsky et al. proposed a control method for handling large flexible objects, where several robots with manipulators grasp them. The robots use their thrusters as a low frequency control of object rigid body motion, while they use their manipulators, via a high frequency control, to cancel out vibrations this motion causes on the flexible bodies [9]. Nevertheless, in several cases, the flexibility of the handled object can be neglected, due to size and low accelerations during the motion. Fitz-Coy and Hiramatsu presented a post-docking control approach based on game theory, minimizing interaction forces, and thus helping avoid the loss of firm grasp [10]. Everist et al. proposed a free-flying servicer concept for handling and assembling space construction rods, using proportional thrusters under PD control [11]. Orbital system thrusters, though, operate under on-off control. Rekleitis and Papadopoulos have proposed the concept of using a number of servicers equipped with manipulators, where both on-off thruster propulsion and manipulator proportional forces/ torques are used in hadling an object, see Fig. 1. Using a uni-dimensional, proof-of-concept model, they demonstrated the advantages of this concept over the one in which servicers without manipulators are used [12]. These include an improvement in handling accuracy and fuel consumption.

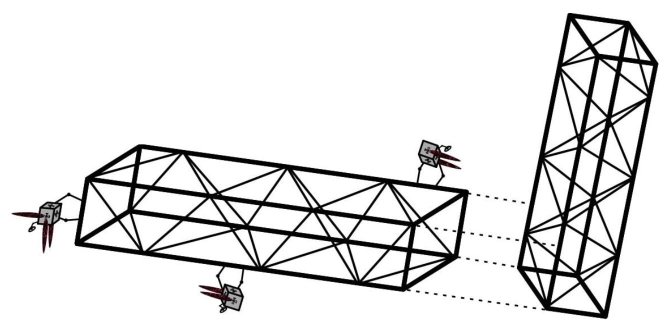

Figure 1. Handling of a rigid passive body by a number of cooperating free-flyers equipped with manipulators, during a space structure assembly.

This work uses this concept to develop a strategy that utilizes both on-off thrusters and manipulator proportional forces/ torques applied by a number of robotic servicers, see Fig. 1, to cancel the effect of limit cycles on the object, and enhance its handling both in terms of accuracy and of fuel consumed. As an example, the paper studies the case of three cooperating single-manipulator free-flying robotic servicers, handling a larger passive rigid body by pushing it with their end effectors, without a firm grasp. To this end, the equations of motion of the system of servicers and object

Georgios Rekleitis and Evangelos Papadopoulos are with the Department of Mechanical Engineering, National Technical University of Athens, Greece (e-mail: [georek, egpapado]@central.ntua.gr; phone: +30-210-772-1440).

are developed and a model based control algorithm is derived. Optimization techniques provide the forces to be applied to the object, while the optimal contact points are found using a higher-level optimization process. Controller performance is shown to exhibit desirable response characteristics, such as remarkable positioning accuracy and limited thruster fuel consumption.

II. Manipulation By Free-Flying Robots

A candidate scenario for handling an object in space is to have servicers without manipulators in contact with it, essentially lending their thrusters to its motion. However, this method can result in limit cycles that increase both position errors and fuel consumption. To eliminate these undesirable effects, we propose the use of servicers with manipulators that apply to the object forces of proportional nature, while the servicer thrusters operate to move the system's center of mass (CM). Thus, the on-off forces of the thrusters are filtered, both by the inertia of the servicer base and by the manipulators, canceling the limit cycle effects on the motion of the passive object. This method results in accurate point-to-point and trajectory tracking control of the object, while the firing of the thrusters is kept limited. The application of the concept was demonstrated via a simplified uni-dimensional system in [12]. Here, the demanding case of tracking a desired trajectory is studied. If the requirements are relaxed to a point-to-point motion, an optimal trajectory can be computed to lower the fuel consumption further.

To control an object in six degrees of freedom (DOFs), three forces and three torques must be exerted on it. If a firm a firm grasp of the object is possible, then handling can be done by a single appropriate manipulator. However, this is not feasible always (e.g. as in the case of orbital debris). In such a case, a manipulator may only be capable of pushing a passive body, introducing a unilateral constraint. In addition, to avoid end-effector slipping, or risking losing the object, the applied forces will have to stay within the friction cone. Taking the above into account, in this work it is assumed that a passive object is handled by free-flying servicers whose manipulator end-effectors apply point contact forces. The analysis and results also apply in the case of firm grasping. Then, no unilateral force constraints apply, while the end-effector forces do not need to be in a friction cone.

To keep the free-flying servicers as simple as possible, single manipulator servicers are assumed. To avoid damaging the passive object, thrusters facing it are off. The mass and inertia of the servicer manipulators are assumed much smaller than those of the servicers or the object, and are neglected for simplicity.

The dynamics of a system of n orbital robotic servicers controlling a rigid passive body via manipulators is studied next. The equations of motion for the passive object (i = 0) and for the free-flying servicer bases (i = 1, …, n), are

$$\mathbf{H}_i \ddot{\mathbf{q}}_i + \mathbf{C}_i\left(\mathbf{q}_i, \dot{\mathbf{q}}_i\right) = \mathbf{Q}_i \tag{1}$$

where $\mathbf{q}_i$ are the generalized coordinates for the object (i = 0) and the servicer bases (i = 1, …, n),

$$\mathbf{q}_i^T = \left[\mathbf{r}_i^T, \boldsymbol{\theta}_i^T\right]^T = \left[x_i, y_i, z_i, \theta_i, \varphi_i, \psi_i\right]^T \tag{2}$$

where, $[x_i\ y_i\ z_i]^T$ is the position vector $\mathbf{r}_i$ of body i and $[\theta_i\ \varphi_i\ \psi_i]^T$ denote the Euler angles $\boldsymbol{\theta}_i$ of the same body. The $\mathbf{H}_i$ are the 6×6 mass matrices of body i, with

$$\begin{aligned}\mathbf{H}_i &= \begin{bmatrix} \mathrm{diag}(m_i, m_i, m_i) & \mathbf{0}_{3x3} \\ \mathbf{0}_{3x3} & \mathbf{E}_i^T \mathbf{R}_i \mathbf{I}_i \mathbf{R}_i^T \mathbf{E}_i \end{bmatrix} = \\ &= \begin{bmatrix} \mathbf{I}_{3x3} & \mathbf{0}_{3x3} \\ \mathbf{0}_{3x3} & \mathbf{E}_i^T \end{bmatrix} \begin{bmatrix} \mathrm{diag}(m_i, m_i, m_i) & \mathbf{0}_{3x3} \\ \mathbf{0}_{3x3} & \mathbf{R}_i \mathbf{I}_i \mathbf{R}_i^T \mathbf{E}_i \end{bmatrix} = \mathbf{E}_i^* \ \mathbf{H}_i^*\end{aligned} \tag{3}$$

where $\mathbf{I}_{3x3}$ is the 3×3 identity matrix, $\mathbf{R}_i$ is the rotation matrix transforming vectors from the frame i to the inertial frame, $\mathbf{I}_i$ and m_i are the inertia matrix and mass of body i respectively, $\mathbf{E}_i$ is a 3×3 matrix mapping the Euler rates $\dot{\boldsymbol{\theta}}_i$ of body i to its angular velocity $\boldsymbol{\omega}_i$:

$$\boldsymbol{\omega}_i = \mathbf{E}_i \dot{\boldsymbol{\theta}}_i \tag{4}$$

$\mathbf{C}_i$ are 6×1 vectors containing the nonlinear velocity terms,

$$\begin{aligned}\mathbf{C}_i &= \left[\ \mathbf{0}_{1x3},\ \left(\mathbf{E}_i^T \mathbf{C}_i^*\right)^T\ \right]^T = \\ &= \left[\ \mathbf{0}_{1x3},\ \left(\mathbf{E}_i^T\left(\mathbf{R}_i \mathbf{I}_i \mathbf{R}_i^T \dot{\mathbf{E}}_i \dot{\boldsymbol{\theta}}_i + \mathbf{E}_i \dot{\boldsymbol{\theta}}_i \times \mathbf{R}_i \mathbf{I}_i \mathbf{R}_i^T \mathbf{E}_i \dot{\boldsymbol{\theta}}_i\right)\right)^T\ \right]^T\end{aligned} \tag{5}$$

and $\mathbf{Q}_i$ ($i = 1,\ldots,n$) are 6×1 vectors that include thruster forces, reaction wheel moments and manipulator forces/ torques acting on the i^{th} servicer base,

$$\mathbf{Q}_i = \begin{bmatrix} \sum_{j=1}^{6} \mathbf{f}_{ij} + \mathbf{f}_{bi} \\ \mathbf{E}_i^T \left(\mathbf{n}_i + \mathbf{n}_{bi} + \sum_{j=1}^{6}\left(\mathbf{f}_{ij} \times \mathbf{d}_{ij}\right) - \mathbf{f}_{bi} \times \mathbf{p}_i\right) \end{bmatrix}, \quad \begin{matrix} i = 1,\ldots,n \\ j = 1,\ldots,6 \end{matrix} \tag{6}$$

where $\mathbf{f}_{ij}$ and $\mathbf{n}_i$ are the thruster forces and reaction wheel torques acting on the i^{th} servicer base respectively, $\mathbf{f}_{bi}$ and $\mathbf{n}_{bi}$ are the forces and torques transmitted to the i^{th} servicer base by its manipulator, $\mathbf{d}_{ij}$ is the vector locating the j^{th} thruster of the i^{th} servicer base with respect to the base CM, and $\mathbf{p}_i$ is the position vector locating the i^{th} manipulator mount with respect to the base CM, see also Fig. 2.

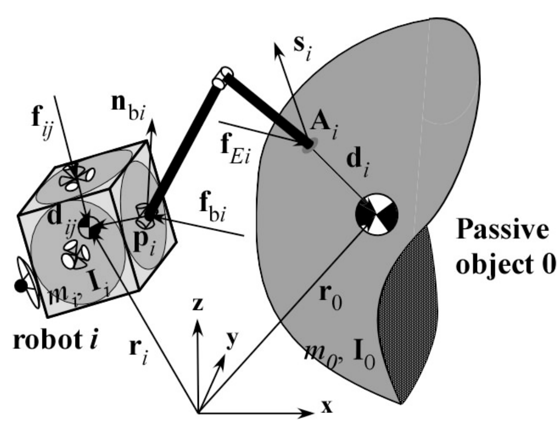

Figure 2. Passive object (0) and the i^{th} free-flyer with a single manipulator.

The vector $\mathbf{Q}_0$ includes forces and moments applied on the passive object by the n end-effectors:

$$\mathbf{Q}_0 = \begin{bmatrix} \sum_{i=1}^{n} \mathbf{f}_{Ei} \\ \mathbf{E}_i^T \sum_{i=1}^{n} \left(\mathbf{f}_{Ei} \times \mathbf{d}_i \right) \end{bmatrix} = \begin{bmatrix} \mathbf{f}_0 \\ \mathbf{n}_0 \end{bmatrix} \tag{7}$$

where $\mathbf{f}_{Ei}$ are the forces applied on the passive object by the i^{th} end-effector, and $\mathbf{d}_i$ is the vector from a contact point $\mathbf{A}_i$ at the passive object to the CM of the passive object.

Combining the above equations for all the $n + 1$ bodies to a single matrix equation, the following is obtained:

$$\mathbf{H}\ddot{\mathbf{q}} + \mathbf{C}\left(\mathbf{q}, \dot{\mathbf{q}}\right) = \mathbf{Q} \tag{8}$$

where:

$$\mathbf{q} = \left[\mathbf{q}_0^T, \mathbf{q}_1^T, \mathbf{q}_2^T, ..., \mathbf{q}_n^T \right]^T \tag{9}$$

$$\mathbf{H} = diag\left[\mathbf{H}_0, \mathbf{H}_1, \mathbf{H}_2, ..., \mathbf{H}_n \right] \tag{10}$$

$$\mathbf{C} = \left[\mathbf{C}_0^T, \mathbf{C}_1^T, \mathbf{C}_2^T, ..., \mathbf{C}_n^T \right]^T \tag{11}$$

$$\mathbf{Q} = \left[\mathbf{Q}_0^T, \mathbf{Q}_1^T, \mathbf{Q}_2^T, ..., \mathbf{Q}_n^T \right]^T \tag{12}$$

Since two manipulators applying point contact forces cannot exert a torque parallel to the line connecting the two contact points, at least three manipulators are needed to handle an object. In the remaining of the paper, it is assumed that the object is handled by the minimum number of manipulators/ servicers, i.e. $n = 3$.

III. Passive Object Force Planning And Control

To control the passive object, the inertial force $\mathbf{f}_0$ and torque $\mathbf{n}_0$ applied, are computed using a model based control law,

$$\left[\mathbf{f}_0^T, \mathbf{n}_0^T \right]^T = \left[\mathbf{0}_{1x3}, \mathbf{C}_0^T \right]^T + \mathbf{H}_0 \left(\ddot{\mathbf{q}}_{0des} + \mathbf{K}_{P0}\mathbf{e}_0 + \mathbf{K}_{D0}\dot{\mathbf{e}}_0 \right) \tag{13}$$

where $\mathbf{e}_0 = \mathbf{q}_{0,\,des} - \mathbf{q}_0$ and $\mathbf{q}_{0,\,des}$ is the desired trajectory for the passive object and $\mathbf{K}_{P0}$ and $\mathbf{K}_{D0}$ are control gains. These forces and torques must be applied by the three end-effectors in contact with the passive object, i.e. by the three $\mathbf{f}_{Ei}$ forces However, the later, are subject to constraints.

Although (1) to (12) also hold in the case of a firm grasp of the passive object, the assumption of point contacts introduces unilateral constraints for the contact forces $\mathbf{f}_{Ei}$. These forces must continuously push the object so that loss of contact is avoided, and in addition must remain within the friction cone of the contacting surfaces, so that slip of the end-effector on the surface of the passive object is avoided. Therefore, the following constraints for $\mathbf{f}_{Ei}$ must hold,

$$\mathbf{-f}_{Ei} \bullet \mathbf{s}_i < 0, \quad i = 1,2,3 \tag{14}$$

$$\text{atan2}\left(\left\| \mathbf{s}_i \times \left(-\mathbf{f}_{Ei} \right) \right\|, -\mathbf{f}_{Ei} \bullet \mathbf{s}_i \right) \leq \text{atan}\left(\mu_i \right), \quad i = 1,2,3 \tag{15}$$

where $\mathbf{s}_i$ is the vector at the i^{th} contact point $\mathbf{A}_i$, perpendicular to the surface of the passive object and facing outwards and μ_i is the corresponding friction coefficient between the two contacting surfaces. In Eq. (15), the function atan2 is used to take into account the direction of $\mathbf{f}_{Ei}$.

As mentioned earlier, thrusters facing the passive object are deactivated for safety reasons. Therefore, no thruster forces are available to push a servicer away from the passive object, if their distance is less than a preset threshold. The task of keeping a base above a threshold distance can be accomplished by its manipulator through the application of an appropriate reaction $\mathbf{f}_{bi}$, see (6). The free-flying robot controller (Section IV) calculates the required repulsive force $\mathbf{f}_{ij\_r}$ to push the servicer away from the object. This force though, is applied as a component of the manipulator reaction $\mathbf{f}_{bi}$. Thus, in order to safely push the servicer, this component of $\mathbf{f}_{bi}$, must be at least equal to the calculated $\mathbf{f}_{ij\_r}$. Since the manipulator dynamics are assumed negligible, $\mathbf{f}_{bi}$ is equal to $-\mathbf{f}_{Ei}$. Thus, the $\mathbf{f}_{Ei}$ is subject to this constraint, too. For example, if the deactivated thrusters for the i^{th} robot are pointing along the u-direction, (16) must hold:

$$\left\{ \mathbf{f}_{bi} \right\}|_{\_u} = -\left\{ \mathbf{f}_{Ei} \right\}|_{\_u} \geq \mathbf{f}_{ij\_r}, \qquad i = 1,2,3 \tag{16}$$

where the notation $|_{\_u}$ denotes a component along the u-direction. In (16), an inequality is used, so as not to over-restrain $\mathbf{f}_{Ei}$, while at the same time to be able to apply at least the desired control force $\mathbf{f}_{ij\_r}$.

Eqs. (7), (13), (14), (15) and (16) must hold for the applied $\mathbf{f}_{Ei}$. Although (13) dictates the force and torque that must be applied to the object, the end-effector forces $\mathbf{f}_{Ei}$ cannot be calculated by equating (7) and (13) due to redundancy and to the existence of constraints. Therefore, at each moment t of the motion of the system, we resort to the use of a constrained nonlinear optimization method, with the nine components of the three end-effector forces $\mathbf{f}_{Ei}$ as the design parameters. The performance index is chosen as,

$$\Lambda_1(t) = \min_{\mathbf{f}_{Ei}} \sum_{i=1}^{3} \left(\mathbf{f}_{Ei}^2 \right) \tag{17}$$

so that the sum of the squared norm of the applied forces is minimized. Eqs. (7) and (14) are linear constraints, while Eqs. (15) and (16) are non-linear constraints to be observed. Through (13), the desired trajectory provides the required generalized forces and the optimization process, returns the contact forces $\mathbf{f}_{Ei}$ that must be applied by the manipulators so that the object trajectory is followed, the norm of the forces is minimized and the constraints observed. The initial guess for each optimization step is the $\mathbf{f}_{Ei}$ of the previous step/ moment, while for the first step, the initial guess is $\mathbf{f}_{Ei} = \mathbf{0}$.

In the above analysis, it was assumed that the contact point locations of the end-effectors were given. However, the solution obtained depends on these locations. A poor choice may result in high end-effector forces and in turn, in excessive servicer thrusting and fuel expenditure. Therefore, it is beneficial to search for optimal contact points. To this end, an additional optimization is set up, having the coordinates of the contact point vectors $\mathbf{d}_i$ as the design parameters. The performance index is now of min-max type,

$$\Lambda_2 = \min_{\mathbf{d}_i} \left(\max_t \Lambda_1(t) \right) \tag{18}$$

where the maximization over time t means that, for a given set of $\mathbf{d}_i$, the trajectory tracking motion is simulated and the overall maximum $\Lambda_1(t)$ over the motion time is obtained. The optimization process then chooses a different set of $\mathbf{d}_i$

until the overall $\max_t \Lambda_1(t)$, i.e. the overall worse force requirement, is minimized during the object desired motion. The procedure finally yields the optimal contact point vectors $\mathbf{d}_i$, subject to geometrical constraints defined by the object geometry. After completing this optimization process, both the optimal contact points and the force profiles for the free-flying robots are known.

IV. Servicer Trajectory Planning and Control

Planning the desired free-flying servicer trajectory is complex, as the manipulator servicer will have to apply the required $\mathbf{f}_{Ei}$ on the passive object while maintaining a desired position and attitude of its base that takes into account workspace and collision avoidance requirements. To this end, an appropriate initial servicer base position and orientation with respect to the passive object are selected. In more detail, it is desired that the base relative position and orientation are maintained within certain safety limits, throughout the object motion. Hence, the desired servicer base trajectory $\mathbf{q}_{ides}$ is computed based on the object trajectory and sent to its motion controller, presented next.

The servicer motion controller takes as feedback the position and attitude of the servicer base and uses it to compute the motion tracking errors, based on its desired trajectory. Employing a model-based controller, the control inputs on a servicer are given by,

$$\left[\sum_{j=1}^{6} \left(\mathbf{f}_{ij}^{\mathrm{T}} \right), \quad \mathbf{n}_i^{\mathrm{T}} \right]^{\mathrm{T}} = \mathbf{H}_i^* \left(\ddot{\mathbf{q}}_{ides} + \mathbf{K}_{Pi} \mathbf{e}_i + \mathbf{K}_{Di} \dot{\mathbf{e}}_i \right) + \mathbf{W}_i \qquad (19)$$

where,

$$\mathbf{W}_i = \left[\quad -\mathbf{f}_{bi}^T, \quad \left(\mathbf{C}_i^* - \mathbf{n}_{\mathrm{b}i} - \sum_{j=1}^{6} \left(\mathbf{f}_{ij} \times \mathbf{d}_{ij} \right) + \mathbf{f}_{bi} \times \mathbf{p}_i \right)^T \quad \right]^T \qquad (20)$$

and $\mathbf{K}_{Pi}$ and $\mathbf{K}_{Di}$ are control gain diagonal matrices, $\mathbf{H}_i^*$ and $\mathbf{C}_i^*$ are defined in Eq. (3) and (5), while $\mathbf{e}_i = \mathbf{q}_{ides} - \mathbf{q}_i$ is the error between the desired $\mathbf{q}_{ides}$ and the actual $\mathbf{q}_i$ and $\mathbf{f}_{\mathrm{b}i}$ and $\mathbf{n}_{\mathrm{b}i}$ are the reaction force and moment transmitted to the i^{th} servicer base by its manipulator.

To apply the controller given by Eqs. (19) and (20), the $\mathbf{f}_{\mathrm{b}i}$ and $\mathbf{n}_{\mathrm{b}i}$ must be available. These are related to the manipulator end-effector force $\mathbf{f}_{Ei}$ by the manipulator force transmission equation,

$$\mathbf{J}_i^T \mathbf{f}_{Ei} = \begin{bmatrix} \mathbf{f}_{\mathrm{b}i} \\ \mathbf{n}_{\mathrm{b}i} \end{bmatrix} \qquad (21)$$

where $\mathbf{J}_i$ is a 6×3 Jacobian-like matrix that is a function of the manipulator posture and that resolves the end-effector force $\mathbf{f}_{Ei}$ to the base reactions. Since the manipulator dynamics were neglected, Eq. (21) yields $\mathbf{f}_{\mathrm{b}i} = -\mathbf{f}_{Ei}$.

Note that if Eqs. (19) and (20) are used as described above, continuous $\mathbf{f}_{ij}$ forces will result. However, current thruster forces are on-off. Thus, a thruster switching strategy is also needed. A simple strategy is to compute the continuous $\mathbf{f}_{ij}$ from Eqs. (19) and (20), transform them to the corresponding servicer base frame, and then turn each thruster on, when the corresponding continuous force value exceeds a preset threshold value f_t. The resulting controller does not lead to asymptotic stability, but this is not a restriction, since all is needed here is error boundedness.

Once the thruster forces $\mathbf{f}_{ij}$ are computed, then the moments $\mathbf{f}_{ij} \times \mathbf{d}_{ij}$ that these forces apply to the base are also computed, and using Eqs. (19) and (20), the reaction wheel torques $\mathbf{n}_i$ are obtained. Since wheel-applied moments are limited (in existing systems by a moment of the order of 1 Nm), larger moments can be applied by employing pairs of on-off thrusters. Then, the continuous $\mathbf{n}_i$ obtained by Eqs. (19) and (20) is also discretized, using the same switching strategy as in the case of $\mathbf{f}_{ij}$, with a preset threshold value n_t.

The computation of the $\mathbf{f}_{ij\_r}$ required to keep the robot away from the passive object, needed in Eq. (16), is obtained employing model-based control. To this end, a control force $\mathbf{F}_{mb}$ is calculated first according to,

$$\mathbf{F}_{mb} = \mathrm{diag}(m_i, m_i, m_i) \left(\ddot{\mathbf{r}}_{ides} + \mathbf{K}_{Di} \dot{\mathbf{e}}_{r\_i} + \mathbf{K}_{Pi} \mathbf{e}_{r\_i} \right) \qquad (22)$$

where $\mathbf{K}_{Pi}$ and $\mathbf{K}_{Di}$ are control gain diagonal matrices, while $\mathbf{e}_{r\_i} = \mathbf{r}_{ides} - \mathbf{r}_i$ is the error between the desired $\mathbf{r}_{ides}$ needed to achieve the desired position control, and the actual $\mathbf{r}_i$ of the servicer, where the $\mathbf{r}_i$ has been defined in Eq. (2). Depending on the sign of $\mathbf{F}_{mb}$'s component along the direction of the deactivated thrusters, the need for the repulsive force $\mathbf{f}_{ij\_r}$ is decided. A negative sign for this component implies the need for a repulsive force, equal to the component of the $\mathbf{F}_{mb}$ along the deactivated thrusters direction. A positive sign implies the need for a force pushing the robot towards the passive object; however, this force can be supplied by the thrusters and therefore in this case, the $\mathbf{f}_{ij\_r}$ should be zero. Then, $\mathbf{f}_{ij\_r}$ is obtained as:

$$\mathbf{f}_{ij\_r} = \begin{cases} \left\{ \mathbf{F}_{mb} \right\}\big|_{\_r} & \text{if } \mathrm{sgn}\left(\left\{ \mathbf{F}_{mb} \right\}\big|_{\_r} \right) < 0 \\ 0 & \text{if } \mathrm{sgn}\left(\left\{ \mathbf{F}_{mb} \right\}\big|_{\_r} \right) \geq 0 \end{cases} \qquad (23)$$

where the symbol $|_{\_r}$ denotes the component along the direction of the deactivated thrusters.

Having obtained $\mathbf{f}_{ij\_r}$, the required end-effector force $\mathbf{f}_{Ei}$ can also be obtained, as shown in Section III, and then the servicer controller of Eqs (19) to (21) computed, see Fig. 3.

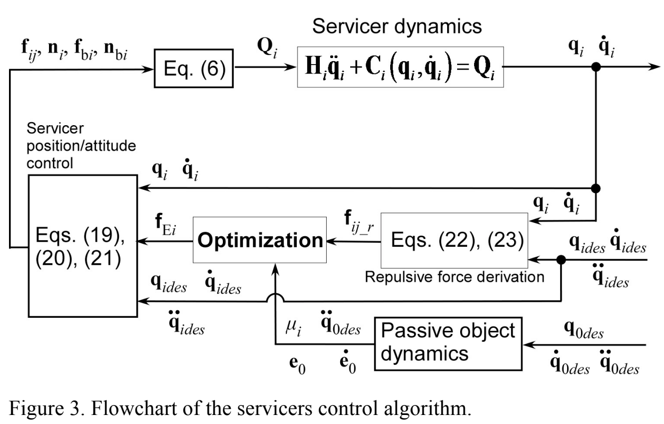

Figure 3. Flowchart of the servicers control algorithm.

V. SIMULATION RESULTS

To demonstrate the methodology described earlier, we study the case of three single-manipulator servicers, applying point contact forces on the passive object (no grasping). Each servicer base has thrusters capable of producing forces or moments, (thrusters facing the object are deactivated), reaction wheels, and a single PUMA-type manipulator.

A series of simulations is run, with realistic parameters in terms of force and torque capabilities of thrusters and reaction wheels. The rigid passive body to be handled has mass of 180 kg in the shape of a 2m×3m×2m orthogonal parallelepiped. The free-flying servicers have mass of 70 kg each, and their base is of cubic shape with a 0.7 m side. The three contact points lie on the object surfaces with normal vectors parallel to the $\hat{\mathbf{x}}_0$, $-\hat{\mathbf{x}}_0$ and $\hat{\mathbf{y}}_0$ unit vectors of the object body-fixed axes. The servicer thrusters develop per axis a pure force of 20 N, while their trigger threshold is set to f_t =10 N. For attitude control, the servicers have additional pairs of thrusters that develop pure torque of 2 Nm per axis, and reaction wheels that can develop proportional torques up to n_t =1 Nm per axis. The manipulator on each robot has a maximum reach of 3 m. The simulations are run on the Matlab/ Simulink package. To obtain $\mathbf{f}_{Ei}$ and the optimal contact points, the *fmincon* non-linear constrained optimization process is employed.

First, a motion of all four bodies is simulated, in which each of the six dof of the passive object follow a trapezoidal profile for the linear velocity or Euler angles rate, see Table I. The servicers' position control task is to keep the manipulator base at a distance equal to 1.5 m, measured along the object surface normal vector passing from the end-effector contact point. The servicers' attitude control task is to keep the surface of the servicer that the manipulator is mounted on, parallel to the corresponding contact surface of the passive object. The control gains in Eq. (13) are K_{P0} = 1.8, K_{D0} = 3.24 (for all passive object *translational* dof), K_{P0} = 0.7, K_{D0} = 0.49 (for all passive object *rotational* dof). The gains in Eq. (19) are K_{Pi} = 0.4, K_{Di} = 0.16 (for all servicer bases *translational* dof) and K_{Pi} = 3, K_{Di} = 9 (for all the *rotational* dof of the servicer bases), with i = 1, 2, 3.

Table I. Passive object desired motion parameters.

dof	const. accel. $(m/s^2)/(rad/s^2)$	up to (s)	const. veloc. (m/s)/ (rad/s)	up to (s)	const. deccel. $(m/s^2)/(rad/s^2)$	up to (s)
x_{0des}	0.0003	56	0.0168	84	-0.0003	140
y_{0des}	-0.00036	50	-0.018	90	0.00036	140
z_{0des}	0.0002	59	0.0118	81	-0.0002	140
θ_{0des}	$5*10^{-5}$	60	0.003	80	$-5*10^{-5}$	140
φ_{0des}	$7*10^{-5}$	55	0.00385	85	$-7*10^{-5}$	140
ψ_{0des}	10^{-4}	65	0.0065	75	-10^{-4}	140

For the object trajectory in Table I, the actual trajectory is displayed in Fig. 4. Fig. 5 shows the object tracking errors, the distance between a manipulator base and the corresponding contact point, and the servicer attitude tracking errors, for one of the servicers. Fig. 6 shows the end-effector applied forces, the servicer thruster forces and torques and reaction wheel torques, for the same servicer. The same variables for the other servicers are similar and are not shown here for brevity. As can be seen in Figs. 4, 5, and 6, the passive body follows its trajectory very well. As shown in Fig. 5c, the error displacements from the desired base location with respect to the object, oscillate around zero, indicating that the manipulator base remains close to the target point. Also, as shown in Fig. 5d, the servicer attitude errors are very small.

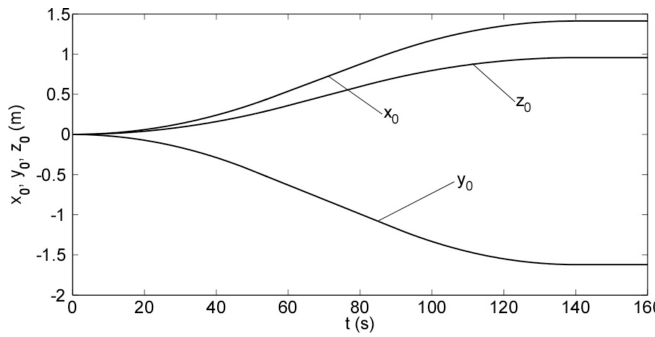

Figure 4. Actual trajectories of the passive object coordinates.

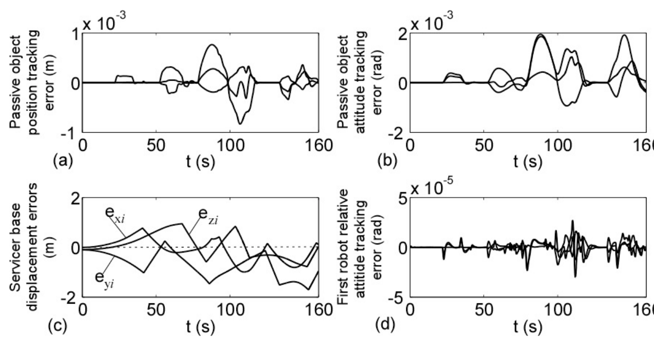

Figure 5. (a) Typical object tracking position errors and, (b) attitude errors. (c) Servicer base displacement errors, and (d) attitude errors.

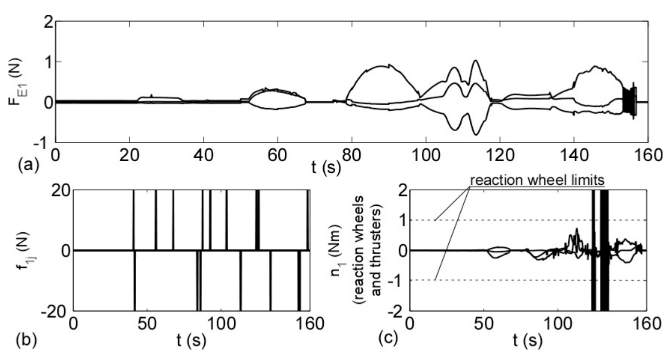

Figure 6. (a) Typical manipulator applied forces, (b) thruster forces and (c) torques by reaction wheels and thrusters for one of the robots.

By increasing the position control gains of the servicer, the error displacements are reduced accordingly. As expected, more frequent thruster firing is observed, thus raising the fuel consumption. This behavior demonstrates how the introduction of the manipulators enhances the performance of the system, letting the servicer base move freely in the manipulator workspace, firing the thrusters only when the manipulator approaches its workspace limits, while constantly applying the proportional manipulator force on the passive object. Thus, the infrequent thruster on-off forces are filtered by the servicer base and the manipulator, resulting in proportional control force on the object. As a result, the thruster forces are quite sparse, see Fig. 6b. The servicer required moments are in general low and are applied by the reaction wheels. In the few moments in which the wheels cannot supply the required moment, the additional set of thrusters fire-up, operating at one-tenth of the thruster maximum propulsion capability.

Another set of simulations was run to compare the performance of the proposed system, to that of a system with pure on-off thrusters firmly attached to the passive object. The fuel consumption was obtained as the integral of all thruster absolute forces. Comparing Figs. 7a, 7c with Fig. 7b, 7d, it can be seen that the performance of the proposed system is superior to that of the pure on-off control, both in terms of fuel consumption and in terms of accuracy.

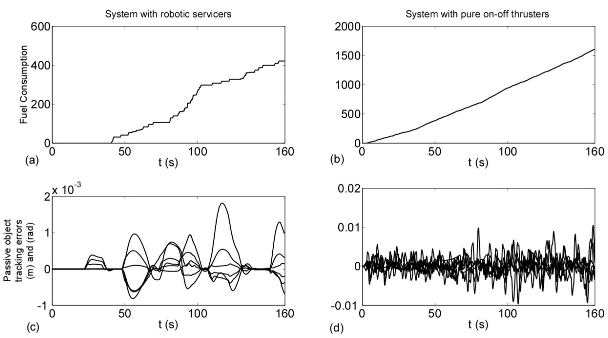

Figure 7. Tracking error as a function of time and corresponding consumed energy. (b), (d) without manipulators, and (a), (c) with manipulators.

A final set of simulations was run to evaluate the controller robustness to parameter variations. Several parametric inaccuracies and failures in the application of some forces were introduced, see Table II, keeping the same controller and gains as before. Fig. 8 displays the same variables as those of Fig. 5. It can be seen that the tracking capability of the system is still remarkable, while the servicers are again within their workspace limits.

Table II. Introduced Inaccuracies

Object mass error	Thruster $\mathbf{f}_{34}$ lag	Thruster $\mathbf{f}_{23}$ lag	Error in force $\mathbf{f}_{E1}$
-20%	0.4 s	0.4 s	-15%

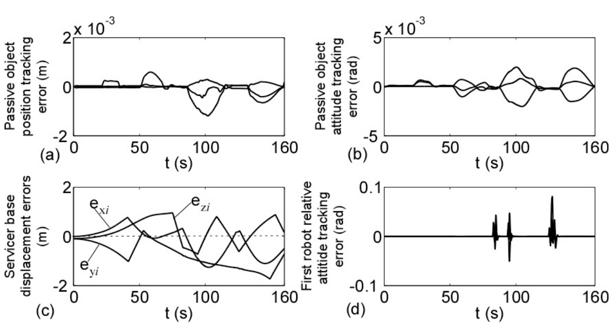

Figure 8. (a) Typical object tracking position errors and, (b) attitude errors. (c) Servicer base displacement errors, and (d) attitude errors.

VI. Conclusions

This work has presented a technique for handling a passive object that uses on both on-off thrusters and manipulator proportional forces to manipulate passive objects on orbit, canceling the effect of limit cycles and reducing fuel consumption. The paper studies the case of three cooperating single-manipulator free-flying robotic servicers, handling a larger passive rigid object without the need to firmly grasp it. Using a two-layer optimization process, a planning strategy for the trajectory-tracking motion of a passive object including optimal end-effector contact point selection, has been developed, while the manipulation strategy was illustrated using a 3D scenario. A model-based controller adapted to the special characteristics of the system was also presented. The performance of the proposed handling technique is shown to be promising and to exhibit desirable response characteristics, such as remarkable positioning accuracy, while it limits excessive thruster fuel consumption, since it avoids thruster chattering.

References

[1] Tatsch, A., Fitz-Coy, N., and Gladun, S., "On-orbit Servicing: A Brief Survey," *Performance Metrics for Intelligent Systems Conf.*, Gaithersburg, MD, August 15 - 19, 2006.

[2] Rekleitis I., Martin E., Rouleau G., L'Archevêque R., Parsa K., and Dupuis E., "Autonomous Capture of a Tumbling Satellite", *Journal of Field Robotics*, Special Issue on Space Robotics, 2007, Vol. 24, No. 4, pages 275-296.

[3] Kaiser C., Rank P., Krenn R., "Simulation of the Docking Phase for the SMART-OLEV Satellite Servicing Mission", *i-SAIRAS: Int. Symposium on Artificial Intelligence, Robotics and Automation in Space*, Hollywood, USA, February 26-29, 2008.

[4] Yoshida K., "ETS-VII Flight Experiments For Space Robot Dynamics And Control", *Int. Symposium on Experimental Robotics*, Waikiki, Hawaii, USA, December 10 – 13, 2000.

[5] http://www.darpa.mil/orbitalexpress/

[6] Caccavale F., Chiacchio P., "An experimental set-up for cooperative manipulation based on industrial manipulators", *Industrial Robot: An Int. Journal*, 2000, Vol. 27, No. 2, pp. 120-130.

[7] Matsumoto S., Wakabayashi Y., Ueno H., Nishimaki T., "System Analyses and Feasibility Studies for Hyper-OSV (Orbital Servicing Vehicle)", *i-SAIRAS: Int. Symposium on Artificial Intelligence, Robotics and Automation in Space*, Canadian Space Agency, St-Hubert, Quebec, Canada, June 18-22, 2001.

[8] Yoshida K., Nakanishi H., "The TAKO (Target Collaborativize) Flyer: a New Concept for Future Satellite Servicing", *i-SAIRAS: Int. Symposium on Artificial Intelligence, Robotics and Automation in Space*, Canadian Space Agency, Quebec, Canada, June 18-22, 2001.

[9] Dubowsky S., Boning P., "The Coordinated Control of Space Robot Teams for the On-Orbit Construction of Large Flexible Space Structures" *Int. Conf. on Robotics and Automation (ICRA) Special Workshop on Space Robotics*, Rome, Italy, April 2007.

[10] Hiramatsu T., Fitz-Coy N., "Game Theoretic Approach to Post-Docked Satellite Control", *20th Int. Symposium on Space Flight Dynamics*, Goddard Space Flight Center, September 24, 2007.

[11] Everist J., Mogharei K., Suri H., Ranasinghe N., Khostnevis B., Will P., and Shen W., "A System for In-Space Assembly", *2004 IEEE/RSJ Int. Conf. on Intelligent Robots and Systems*, Sendai, Japan., 2004.

[12] Rekleitis, G. and Papadopoulos, E., "Towards Passive Object On-Orbit Manipulation by Cooperating Free-Flying Robots," *Proc. IEEE International Conference on Robotics and Automation (ICRA '10)*, Anchorage, Alaska, May 2010.